Dual process coding of recalled location in human oscillatory brain activity

Mary H. MacLean[1,2]

Tom Bullock[1,2]

Barry Giesbrecht[1,2,3]

[1]Psychological & Brain Sciences, University of California Santa Barbara

[2]Institute for Collaborative Biotechnologies, University of California Santa Barbara

[3]Graduate Program in Dynamical Neuroscience, University of California Santa Barbara

Abstract

A mental representation of the location of an object can be constructed using sensory information selected from the environment and information stored internally. Human electrophysiological evidence indicates that behaviorally relevant locations, regardless of the source of sensory information, are represented in alpha-band oscillations suggesting a shared process. Here we present evidence for two distinct alpha-band based processes that separately support the representation of location, exploiting sensory evidence sampled either externally or internally.

Introduction

Mental representations of behaviorally relevant visual features and locations are based on information sampled from the environment and can persist in visual short-term memory (VSTM) even in the absence of maintained external sensory input (Foster, Sutterer, Serences, Vogel, & Awh, 2016; Harrison & Tong, 2009; Serences, Ester, Vogel, & Awh, 2009). Unlike features (e.g. colors), so long as there is visual input from the environment the location of a stimulus remains available to be selected from that input, in addition to being maintained in VSTM, even if the stimulus is not present. However, uninterrupted visual input is not necessary for successful recall of location, as multiple attended locations can be recalled when eyes are closed during retention (Pearson & Sahraie, 2003). Thus, mental representations of locations can be constructed from information sampled from the external environment or from information encoded internally.

Both the selection and retention of mental representations of locations, regardless of the source of information (i.e., external or internal), appear to be supported by processes associated with alpha band oscillations (Foster et al., 2016; Foster, Sutterer, Serences, Vogel, & Awh, 2017; Kelly, Lalor, Reilly, & Foxe, 2006; Samaha, Sprague, & Postle, 2016; Thut, Nietzel, Brandt, & Pascual-Leone, 2006; van Moorselaar et al., 2018). The retention of spatially selective representations, and the associated alpha activity, may represent a continuous process of selection, i.e., the focus of attention (Lewis-Peacock, Drysdale, Oberauer, & Postle, 2012), VSTM, or a combination of both. More recent evidence suggests that alpha is a unitary mechanism for spatial selectivity shared by attention and VSTM (van Moorselaar et

al., 2018). Here we present evidence that at least two distinct processes associated with alpha-band oscillations support spatially selective representations: (1) a fast and continuous location selection process that is disrupted by a masking stimulus and that degrades without continued external visual input, and (2) a delayed process that emerges when external visual input is no longer available.

Participants (n = 18) performed a delayed spatial estimation task (Foster et al., 2016; Wilken & Ma, 2004; Zhang & Luck, 2008), in which a single stimulus was briefly presented in the periphery, in one of eight possible locations on the circumference of an imaginary circle (**Fig. 1a**). Participants were instructed to attend covertly to the stimulus location, remember its location, and report the location after a short delay. The presence or absence of a masking checkerboard after the stimulus, and the state of the eyes during retention (open or closed) yielded four within-subject conditions: eyes open, eyes open + mask, eyes closed, eyes closed + mask.

Results

Location report precision and guess rate are affected by eye closure

The precision of the reported stimulus location was reduced when participants were required to close their eyes (BF > 1,000), an effect enhanced by the presence of a mask (BF > 1,000; **Fig. 1b**). This suggests that the representation of location without the support of continued external visual input is less precise, especially when masked. While guess rate was extremely low in all conditions, there was a small decrease in guessing when participants were required to close their eyes during retention (BF > 7). Modulation of recall precision by eye closure is inconsistent with evidence that spatial recall, when measured as accuracy, is robust

to eye closure without saccades (Pearson & Sahraie, 2003); however a continuous report measure, as in the case of the delayed estimation task used here, is possibly more sensitive to the effects of eye closure than discrete measures.

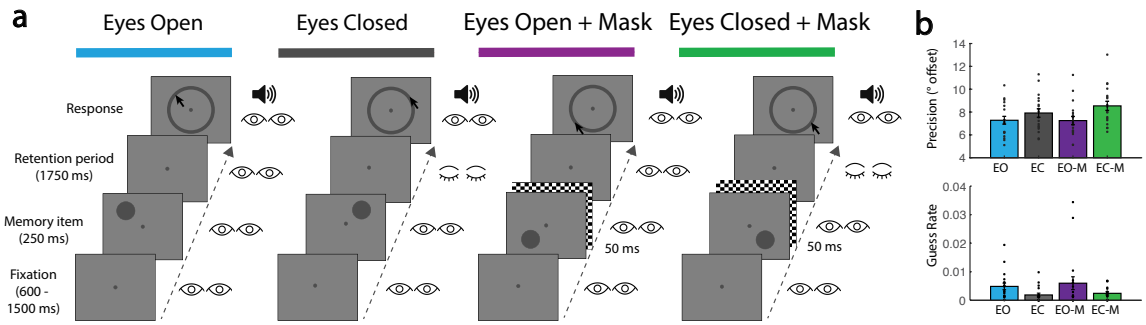

Figure 1. Delayed spatial estimation task. **(a)** Trial procedure for each experimental condition. **(b)** Precision of spatial estimation and guess rate. Error bars = standard error of the mean.

Reconstructions of location representations are temporarily disrupted by a visual mask, and degrade over time with eye closure

In order to observe the spatially selective representation of the stimulus location, an inverted-encoding model (IEM) was employed to reconstruct spatially selective neural population responses from topographically specific patterns of alpha band oscillations in scalp-recorded EEG (Foster et al., 2016; Samaha et al., 2016; van Moorselaar et al., 2018) (**Fig. 2a-c**). More specifically, the IEM method used here employed a general linear model in which the topographic pattern of oscillatory activity was regressed onto an a priori defined set of spatially selective channels. The resulting regression weights, trained and tested using leave-one-out cross-validation, reflect the pattern of neural activity particular to each spatially selective channel. The product of the weights and the observed neural activity yields an estimate of the spatially selective neural response – i.e., the representation of location.

There was evidence of a spatially selective response, centered on the stimulus location, in the alpha band following stimulus presentation under all conditions. The spatially selective response emerged ~200 ms after stimulus onset, around the time when initial effects of covert shifts in spatial attention have previously been observed in evoked activity (Di Russo, Martínez, & Hillyard, 2003; Hillyard et al., 1999).

The presentation of a masking stimulus disrupted the spatially selective response beginning ~200 ms after mask onset (see slope difference between masked and unmasked conditions during the .25-.75s time window in **Fig. 2b** and the corresponding BF for the effect of mask **Fig. 2d "mask"**). An evoked potential observed at parietal and occipital electrode sites, phase-locked to the onset of the mask, was observed to coincide with this disruption (**Fig. 2e**; see **S1** for additional data regarding the role of the stimulus-evoked potential in this disruption). The magnitude of the mask-evoked response predicted the magnitude of disruption to the spatially selective response shortly after mask onset (r (16) = -.66, BF > 10, and r (16) = -.76, BF > 300, for EC+M and EO+M respectively). However, this disruption was neither complete nor permanent. While degraded, evidence for a spatially selective response remained strong following the mask and returned to similar levels observed in the absence of a mask ~500-700 ms after mask onset. This pattern suggests that while a mask disrupts the retention of a spatially selective representation, the representation can be recovered, even in the absence of external visual input.

Unlike the effect evoked by the mask, there was no evidence that the spatially selective response was disrupted by eye closure (**Fig. 2d "eyes"**). Neither did eye closure evoke a phase-locked response (**Fig. 2e**). There was, however, moderate evidence of a small reduction of the spatially selective response later in the retention interval ~1,000 ms after eye closure, as compared to when eyes remained open. Nonetheless evidence for the spatially selective representation remained robust throughout the retention interval when eyes were closed. Thus, the disruptive effect induced by eye closure on spatially selective representations is smaller and delayed compared to the immediate disruptive effect of the mask.

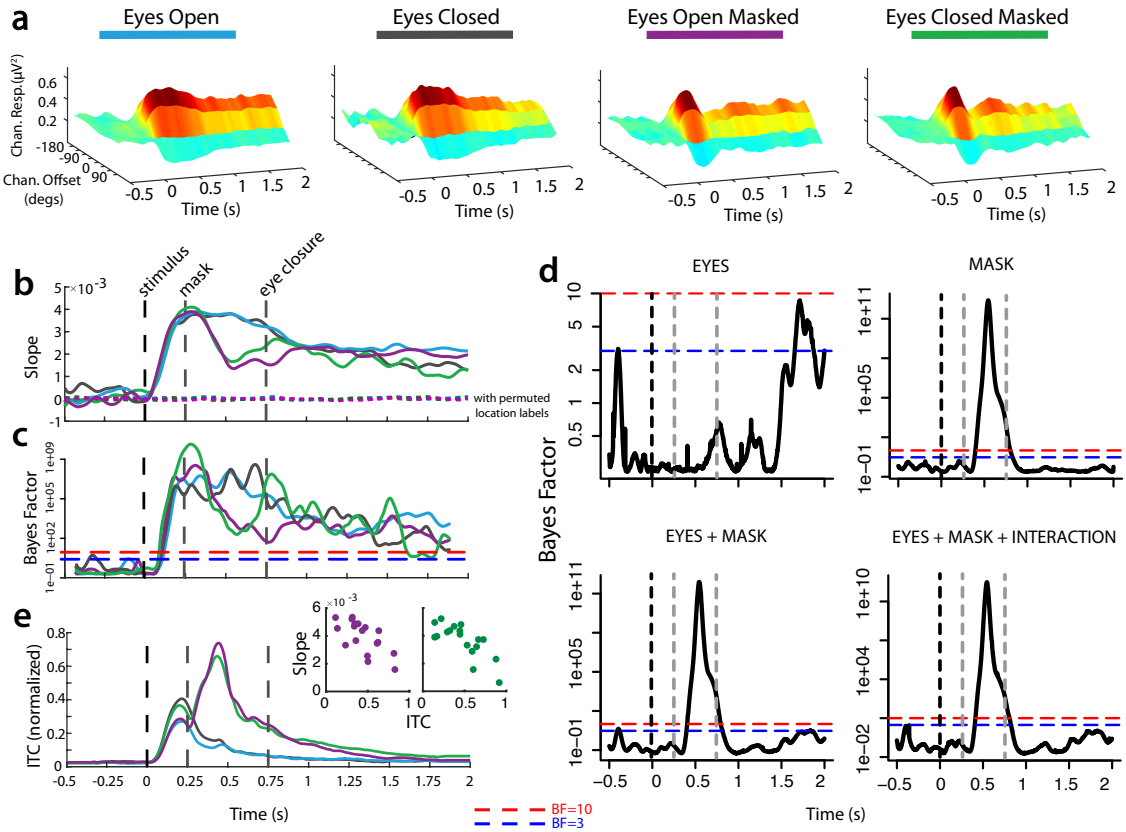

Figure 2. Results of the alpha-based inverted encoding model estimation of the stimulus location. **(a)** Estimated neural population response, or "channel" (offset of channel's preferred location from stimulus location: ±0,45,90,135, or 180°), response (alpha-band power) starting 500 ms before onset of stimulus until end of retention period. **(b)** Linear regression weights of estimated channel response

folded around 0° offset ("slope"), indicating the degree of spatial selectivity. **(c)** Bayes Factor (BF) of t-test comparing slope at each time point to slope of response estimated using permuted location labels. **(d)** BF of ANOVA for effects of eye closure and mask on slope. **(e)** Inter-trial coherence (ITC) indicating stimulus- and mask-evoked potentials and scatterplots of correlation between ITC and slope during the period of the mask-evoked potentials for masked conditions.

Reconstructions of location representations are supported by dual processes

The retention of a spatially selective representation, and its disruption by a masking stimulus, is evident in alpha band oscillations under conditions both with and without continued external visual input. Thus, the patterns of alpha band oscillations that encode for location are persistently robust throughout the entire stimulus presentation and retention interval regardless of condition. However, it is unclear whether a) the continuous encoding of location in alpha band oscillations is supported by a single common process or by multiple distinct processes, and b) which process or processes supporting the spatially selective response are affected by the disruption of external visual input.

In order to observe the dynamics of the process, or processes, supporting spatially selective representations under these different conditions we examined the inter-temporal and inter-conditional generalization of the IEM. The generalization approach can be used to identify the extent to which specific neural codes, reconstructions of spatial spatially selective responses in this case, are present across time and/or conditions (King & Dehaene, 2014). Models of neural codes trained on the topographic pattern of neural activity in specific time windows and/or conditions that can recover similarly reliable spatially selective patterns in other time windows and conditions would be those that exhibit generalization. Such a pattern would be evidence for a common process. In contrast, models trained on

the topographic pattern of neural activity in specific time windows and/or conditions that fail generalize would be evidence that the spatially selective representation is coded by a different topographic pattern of neural activity, i.e. a different process. In the case where a lack of generalization is observed, it is important to rule out the possibility that the impaired ability of the models to reconstruct spatially selective patterns in other time windows and/or conditions is not merely due to reduced data quality (i.e., low signal-to-noise ratio). Importantly, there was evidence of a spatially selective response at all time points in all conditions beginning ~ 200 ms after stimulus onset, thus any lack of generalization can not be attributed to a loss of the signal that encodes for location during these times in any of the conditions.

There was strong evidence of a unitary process supporting the spatially selective response during both stimulus presentation and retention intervals with continuous external visual input when eyes were open and no mask was presented (**Fig. 3a "Train EO → Test EO"**), as there was extensive temporal generalization both forward and backward in time. This pattern is consistent with the conclusion that the process maintaining the spatially selective representation during retention when eyes were open is also the same process as during stimulus presentation (i.e., during selection), and remains static throughout the entire retention interval.

Despite a similarly continuous and robust encoding of location, this was not the case without continuous visual input, when eyes were closed (**Fig. 3a "Train EC → Test EC"**). Earlier time points did not generalize forward in time, nor did later time points generalize backward in time despite evidence for spatially selective

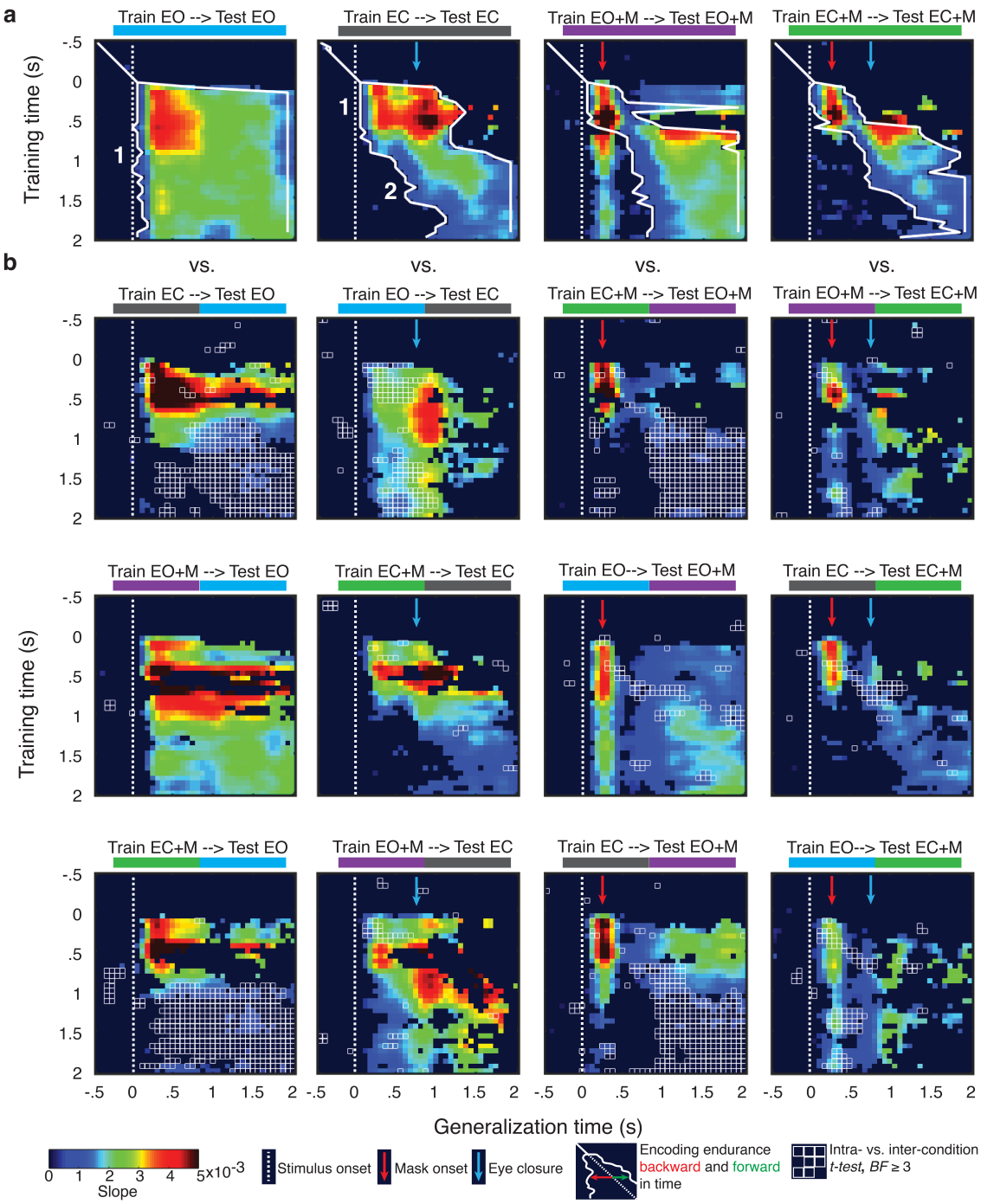

Figure 3. IEM generalization. **(a)** Temporal generalization within experimental condition. Slopes for a spatially selective response are plotted. Those with less than moderate evidence (BF<3) plotted as uniform dark blue. Encoding endurance indicates the sequential extent of temporal generalization backward and forward in time, where BF ≥ 3**.** Process 1 and 2 are indicated in the EO and EC plots. **b)** Inter-condition generalization. Points with moderate or greater evidence (BF ≥ 3) for a difference between intra-condition generalizations shown in Panel A and inter-condition generalizations are outlined in white.

responses at those times. Instead, when eyes were closed the pattern of temporal generalization supports a series of two processes: (process 1) a robust selection process beginning ~100 ms after cue onset and persisting until ~500 ms after eye closure before decaying; and (process 2) a subsequent process, starting around the time of eye closure (~500 ms after stimulus onset) and lasting the remainder of the retention interval.

Process 1 is interrupted in the period following the presentation of a mask in both the eyes open and closed conditions (**Fig. 3a "Train EO+M → Test EO+M"/ "Train EC+M → Test EC+M"**). With eyes open, process 1 re-emerges ~200 ms post-mask, but fails to re-emerge with eyes closed. This pattern of generalization indicates that process 1, a spatial selection process, is dependent on uninterrupted external visual input, is disrupted by a visual masking stimulus, and can be fully recovered when external visual input remains available post-mask (i.e., when eyes remain open). This is similar to the observation that a subsequent cue can restore degraded representations (Sprague, Ester, & Serences, 2016), however, in the current case, there is spontaneous recovery with no aid of additional cues to location.

There was strong evidence that process 1 generalized between eyes open and eyes closed conditions, regardless of mask presence (**Fig. 3b**). Process 1 persisted robustly forward in time towards the end of the retention interval in the eyes open conditions (**"Train EC → Test EO"/ "Train EC+M → Test EO+M")**, but not in the eyes closed conditions (**"Train EO → Test EC"/ "Train EO+M → Test EC+M"**). Although evidence for generalization between eyes open and eyes closed

conditions was stronger and more consistent in the unmasked conditions, process 1 still generalized between masked and unmasked conditions whether eyes were open or closed. This pattern suggests that process 1, the process that overlaps with stimulus processing, is common to all conditions.

Unlike process 1, there was only sporadic, weak evidence that process 2, which supported the representation of spatial selectivity during the retention period when eyes were closed, generalized to the same period when eyes were open. This may indicate that process 2 is not entirely exclusive of conditions with continuous external visual input. However, there is evidence that process 2 generalized between the eyes closed and eyes closed masked conditions. This pattern of generalization indicates that process 2 emerges reliably when there is an interruption to external visual input, as when the eyes are closed.

Changes in alpha, if unrelated to the code for the spatially selective representations, are insufficient to disrupt temporal generalization

Eye closure results in a well-documented increase in alpha power that is not uniformly distributed, rather it is larger at posterior electrodes relative to frontal and temporal electrodes (Barry, Clarke, Johnstone, Magee, & Rushby, 2007; Chapman, Armington, & Bragdon, 1962). Here, as expected, alpha power increased with eye closure (see **S2**) and this increase in power was localized primarily in parietal and occipital electrodes (i.e., over visual cortex). Importantly, these electrodes also carry the greatest weight in the IEM (see **S3**). Thus, it is reasonable to hypothesize that the changes in alpha power and/or topography resulting from eye closure perturbed the coding of the spatially selective representation in alpha and its ability to generalize across time and conditions. However, it is important to

note that not all changes in alpha power and/or topography could affect the spatially selective representation as estimated using the IEM or its generalization. In order for the changes in alpha that accompany eye closure (or the presentation of a mask) to disrupt temporal generalization of the IEM model, those changes have to themselves interact with (i.e., correlate with) the particular pattern of alpha power that codes the spatially selective representation. Importantly, if one simulates the changes in alpha power and topography in the eyes open condition to resemble that of the eyes closed condition during the retention interval as noise, the results of the temporal generalization are unchanged (see **S2** for the results of this simulation). This simulation supports the conclusion that changes in alpha power and topography that are layered on top of the patterns of alpha oscillations coding remembered locations, but are otherwise independent of the memory activity, are insufficient to disrupt the IEM reconstructions of remembered locations and their generalization.

Discussion

Based on the collection of evidence presented here we suggest that mental representations of stimulus location are retained via at least two distinct processes coded in alpha band oscillations. When visual input continues to be available, spatially selective representations can be supported and even recovered by the same process present when a location is initially selected and may be mediated by "attention-based rehearsal" (Awh et al., 1999; Awh, Jonides, & Reuter-Lorenz, 1998; Postle, Awh, Jonides, Smith, & D'Esposito, 2004) of the *external* sensory environment, as has previously been observed (Foster et al., 2016, 2017; van

Moorselaar et al., 2018). However, when visual input is not available, a process possibly based on *internal* selection from information encoded in memory (Chun, Golomb, & Turk-Browne, 2011; Kiyonaga & Egner, 2013) emerges to support the ongoing spatial representation. To the extent that the topographic pattern of alpha oscillations is reflective of the activity in retinotopically mapped brain regions (de Munck et al., 2007; Kelly et al., 2006; Worden, Foxe, Wang, & Simpson, 2000), then our results suggest that these areas are differentially activated when eyes are closed than when eyes are open. This differential involvement may be the result of local changes in patterns of activity (e.g., local patterns of inhibitory activity) or from perturbations from other brain areas (e.g., parietal and/or frontal cortex).

Methods

Participants

Participants were 18 adult volunteers (mean age = 20.8 years, 13 females, all right handed) recruited from the University of California Santa Barbara community. Participants were compensated at a rate of $10 per hour (minimum of $120 total/participant). All participants reported normal or corrected-to-normal vision. The UCSB Human Subjects Committee approved all procedures.

Stimuli and procedure

Each participant completed four testing sessions on four separate days. Sequential sessions were separated by a minimum of 24 hours and a maximum of 1 week. All four sessions were completed within an eight-week period for a given participant. In each session the participant was required to perform 15 blocks of 64 trials (960 trials total) of the same delayed spatial estimation task. Each session

consisted of a different experimental condition of the task: “eyes open” (EO), “eyes closed” (EC), “eyes open with mask” (EO+M), “eyes closed with mask” (EC+M). The order of experimental conditions was counterbalanced between participants.

Each trial of the delayed spatial estimation task began with a small blue fixation dot (subtending 0.2° visual angle) in the center of the screen, along with a green dot (subtending 0.4° visual angle) representing the location of the participant’s gaze. The participant aligned their gaze dot with the fixation dot and pressed the space bar to start the trial. The fixation dot immediately turned grey to indicate that the trial was underway. After a brief fixation (jittered randomly between 0.6 s and 1.5 s) the stimulus, a grey target circle (subtending 1.6° visual angle), appeared, centered at a point on an imaginary circle circumventing 4° from fixation. The stimulus appeared within one of eight angular location bins relative to fixation [0°, 45°, 90°, 135°, 180°, 225°, 270°, 315°], with angle jittered randomly within each bin between +1-44°.

The stimulus remained on screen for 0.25. s. Following stimulus offset there was a 1.75 s retention interval. A grey response ring then appeared, circumventing 4° of visual angle from fixation, along with an auditory cue (0.1 s, 250 Hz pure sine-wave). The participant used the mouse cursor to indicate the location of the target on the response ring. The mouse cursor appeared in a randomized corner of the response screen on each trial. This prevented the participant from anticipating the forthcoming mouse movement during the retention period. The key manipulations between sessions occurred immediately post-stimulus, during the retention interval. In the EO condition participants were instructed to maintain fixation for

the duration of the retention interval. In the EC condition participants were instructed to close their eyes immediately after stimulus offset and reopen them when they heard an auditory cue at the end of the retention interval. In the EO+M and EC+M conditions participants were given then same respective instructions, however the target was masked with a global checkerboard (0.05 s, whole screen, each checker subtending 0.48° by 0.48° of visual angle).

Gaze-contingent eye tracking was employed in all sessions during fixation, stimulus presentation and retention periods. Trials where participants blinked or their gaze deviated more than 2.4° from fixation were aborted. In the EC/EC+M conditions, the trial was also aborted if the participant did not close their eyes between 0.05 s and 0.5 s following target offset. This ensured that participants closed their eyes in a timely manner and also that they viewed the checkerboard mask in its entirety in the masked condition. If the participant reopened their eyes during the retention period of the EC/EC+M condition the trial was aborted. On all trials where the gaze-contingent conditions were broken, the next trial began immediately and the aborted trial was added to the end of the trial sequence for that block of trials, thus ensuring a complete set of trials without gaze deviations were recorded for each participant in each condition.

While performing the task the participant was positioned in a chin rest at 120 cm viewing distance from a monitor (19 inch ViewSonic E90f CRT), and stimuli were presented using custom scripts that utilized the Psychophysics Toolbox for MATLAB. An eye-tracker (Eyelink 1000 plus, SR Research Ltd, Mississauga, Ontario, Canada) was positioned 60 cm from the right eye (monocular tracking @ 1000 Hz,

mean error < 1°). Performance on the delayed spatial estimation task was modeled using the MemToolbox (Foster, Sutterer, Serences, Vogel, & Awh, 2016; Suchow, Brady, Fougnie, & Alvarez, 2013; Zhang & Luck, 2008). A standard mixture model with bias was applied to error in the spatial estimates (in degrees of offset) of each participant within each condition yielding a measure of precision of estimation as well as guess rate.

EEG Data Acquisition

EEG data were recorded for each participant using a BioSemi Active Two system (BioSemi, Amsterdam, Netherlands) consisting of 64 Ag-AgCl sintered active electrodes arranged in an elastic cap (Electro-Cap, USA) and placed in accordance to the 10-20 system. Additional electrodes were placed at the right and left mastoids, as well as 1 cm lateral to the left and right canthi (horizontal) and above and below each eye (vertical) for the EOG. Data were sampled at 1024 Hz and referenced offline to the average mastoid signal. At the beginning of each investigation all impedances were < 20 kΩ. All recording took place in an electrically shielded chamber to ensure minimal interference from external sources of electrical noise.

EEG Data Pre-processing

Custom scripts in MATLAB (version 2013b, Massachusetts, The MathWorks Inc.) and using the EEGLAB toolbox (Delorme & Makeig, 2004) were used for offline processing of the EEG data. The continuous data were referenced to the average mastoid signal and then high- and low- pass filtered between 0.1 Hz and 80 Hz, respectively (EEGLAB function *pop_eegfiltnew)*. The Automatic Artifact Removal (AAR) toolbox (Gomez-Herrero et al., 2006) was then used to remove ocular

artifacts associated with eye closure during the EC/EC-M conditions. The data were then resampled at 256 Hz (EEGLAB function *pop_resample*), to reduce computation time and memory demands, then epoched between -0.5 and 2.5 s around the onset of the stimulus and (EEG data for aborted trials were discarded). The data were then visually inspected and noisy electrodes were excluded (mean electrodes excluded [mean ± SEM] = 1.23 ± .36). In order to maintain consistency in the topographic distribution of electrical activity across the scalp, noisy electrodes that were excluded from one condition were also excluded from all other conditions for that subject. Trials exceeding ± 150 μV in remaining electrodes were then excluded (mean trials excluded: 19.21 ± 4.53; EC 17.06 ± 3.15, EO+M 16.27 ± 3.27; EC+M 16.06 ± 4.14).

Inter-Trial Coherence

In order to observe the evoked response to the stimulus, the mask, and eye closure we calculated inter-trial coherence (ITC) of the epoched data in the alpha (8-12 Hz) range (EEGLAB function *erpimage*) for each participant within each condition. ITC reflects the phase coherence of the EEG signal between trials (between 0 and 1, where 0 indicates no coherence and 1 indicates perfect coherence). Increased phase coherence reflects a reset in phase time-locked to an event (stimulus, mask or eye closure onset). This value is determined separately within each electrode. As we were interested in signals evoked by visual processing we averaged the ITC in parietal and occipital electrodes (P07/8, P03/4, O1/2, POz, Oz).

Spectral Analysis

Epoched data were filtered using a 3rd order Butterworth bandpass filter (MATLAB function *butter*) from 8-12 Hz (alpha). A Hilbert transformation (MATLAB function *hilbert*) was then applied to the filtered signal in order to obtain a measure of instantaneous amplitude and phase. The data were then epoched again between -0.5 to 2 s (.5 s pre stimulus to the end of the retention period).

Prior to modeling, induced power was calculated as the square of the absolute of the Hilbert transformed complex values. Induced power reflects ongoing oscillatory activity regardless of its phase relationship with stimulus onset. Within each location bin trials were then randomly subdivided into three samples and then averaged to create three averaged trials per location bin. Following averaging, each condition included 24 averaged trials (8 location bins x 3 averaged trials).

Because trial based artifact rejection results in uneven numbers of trials per condition, it was necessary to ensure that any comparisons between conditions were not influenced by unequal trial counts. Prior to entering the data into the IEM, the minimum number of trials per location bin (*n)* was calculated across the four conditions for each participant. To ensure equal numbers of trials from each location bin were entered into the model, *n*-1 trials were randomly selected from each bin.

Inverted Encoding Model

An IEM was used to estimate spatially selective neural population ("channels") response profiles based on the topographical distribution of alpha power across the scalp (Foster et al., 2016). The model first estimates the extent to which the linear combination of a priori canonical channel responses (i.e. a basis

set) captures the underlying structure of the observed data (topographical distribution of alpha power), yielding a set of regression weights. The model then uses these weights to estimate the channel response from the observed data. The parameters of these channel response estimates can then be used to quantify the spatially selective response. This method was initially applied to fMRI data (Brouwer & Heeger, 2009, 2011, 2013; Ester, Sprague, & Serences, 2015; Naselaris, Kay, Nishimoto, & Gallant, 2011; Serences & Saproo, 2012) and has been recently applied to EEG recorded at the scalp (Bullock, Elliott, Serences, & Giesbrecht, 2017; Foster et al., 2016; Foster, Sutterer, Serences, Vogel, & Awh, 2017; Garcia, Srinivasan, & Serences, 2013; Samaha, Sprague, & Postle, 2016).

The IEM was run separately for each sample in time (256 Hz EEG sampling rate x 2.5 sec = 640 samples) using induced alpha power within each condition for each participant[1]. For cross-validation of the IEM a *k*-fold approach was employed where $k = 3$. The averaged trials were randomly grouped into three blocks, each with one averaged trial per location bin. Training was performed using 2/3 blocks and the resulting model was tested on the remaining block. This was repeated such that each block served as the test block.

For each participant and condition, m represents the number of EEG electrodes in each dataset (mean across participants = 62.77 ± .36; equivalent within participant), n_1 represents the number of trials in the training set (2 blocks of 8 trials) and n_2 represents the number of trials in the testing set (1 block of 8 trials).

---

[1] Evoked power was also modelled; the results replicated those of Foster et al. (2016), and did not differ by condition.

Let j be the number of hypothetical location selective channels (C_1, j x n_1), composed of half-sinusoidal functions raised to the seventh power as the basis set. Here, the basis set was comprised of 8 equally spaced locations (i.e. j=8). B_1 (m x n_1) represents the training set and B_2 (m x n_2) the test set. A standard implementation of the general linear model (GLM) was then used to estimate the weight matrix (W, m x j) using the basis set (C_1). More specifically, using the GLM:

$$B_1 = WC_1 \qquad \text{(Equation 1)}$$

Then, the ordinary least-squares estimate of W can be computed as:

$$\widehat{W} = B_1 C_1^T (C_1 C_1^T)^{-1} \qquad \text{(Equation 2)}$$

Using the estimated weight matrix ($\hat{W}$, **Equation 2**) and the test data (B_2), the channel responses C_2 (j x n_2) can be estimated by:

$$\hat{C}_2 = (\widehat{W}^T \widehat{W})^{-1} \widehat{W}^T B_2 \qquad \textbf{(Equation 3)}$$

After the $\hat{C}_2$ was solved for each location bin, the channel response function on each averaged trial was then circularly shifted to a common stimulus-centered reference frame (degrees of offset from channel's preferred location bin), and the centered response functions were averaged across channels. The model was repeated for each time sample. To safeguard that the outcome of the model and ensure that any subsequent analyses were not influenced by an idiosyncratic selection of trials, this process was repeated 10 times, with a randomized selection of trials entered into the IEM for each of the iterations, and the final centered tuning function was computed by averaging over the 10 iteration.

The IEM procedure was also performed with randomly permuted location bin labels. Randomizing the location bin labels should eliminate spatially selective

responses and result in flat channel response profiles. These permuted responses were used in hypothesis testing.

Temporal Generalization of IEM

In order to observe the intra- and inter-condition temporal generalization of the IEM we ran the IEM as described above by training at each sample in time, but then testing on every sample in time, either within condition or between conditions. In order to reduce computation time and the number of comparisons we down-sampled the data prior to modeling from 256 Hz (640 samples) to 16 Hz (40 samples). We repeated the generalization IEM procedure with permuted location bin labels for the purpose of hypothesis testing.

Quantifying Spatially Selective Representations

To quantify spatial selectivity the estimated channel responses were folded around 0° of offset, transforming the responses from [-135, -90, -45, 0, 45, 90, 135, 180] into [0, 45, 90, 135, 180] by averaging the response at corresponding offsets (± 45, 90, and 135°; 0° an 180° were not averaged). Slope was then computed (MATLAB function *polyfit*) as the linear regression weight of alpha power across offset. Larger slope values indicate greater spatial selectivity.

Hypothesis Testing

Bayes Factor (BF) was calculated for the purpose of inferential statistics (Kass & Raftery, 1995; Kruschke & Liddell, 2016; Rouder, Morey, Speckman, & Province, 2012) using functions from the BayesFactor toolbox for R(Morey, Rouder, & Jamil, 2015), which employs a Cauchy prior. According to various guidelines a BF between 1-3 indicates “anecdotal evidence” for H1, between 3 and 10 indicates

"moderate" evidence, between 10 and 30 indicates "strong" evidence and greater than 30 indicates "very strong" evidence (Dienes, 2016; Kass & Raftery, 1995; Kruschke & Liddell, 2016; Wetzels et al., 2011).

To test the reliability of the spatially selective channel responses, BF paired t-tests (R function *ttestBF*) were computed at each sample in time comparing the slopes of the real and permuted channel response estimates. To test for differences in slope between conditions BF ANOVAs (R function *anovaBF*) with the factors eyes (open vs. closed) and mask (masked vs. unmasked) were computed comparing the slopes of the real channel response estimates at each time point. To contrast slope values resulting from the temporal generalization analyses within conditions, to those between conditions, BF paired t-tests were also computed for each cell in the generalization matrix. To assess the relationship between slope and ITC, BF regressions (R function *regressionBF*) were computed. BF ANOVAs and t-tests were also used to test for differences in performance.

Our analyses involve repeated comparisons at multiple time points, which raises the specter of increased inferential error. However, it should be noted that Bayesian inference, even without correcting for multiple comparisons, is more conservative than frequentist inference, and much less likely to result in false confidence(Gelman & Tuerlinckx, 2000). Furthermore, our effects are present at multiple time points, as hypothesized, and no inference relies on a single comparison, but rather a pattern of effects across time. Our inferences are further strengthened by our use of IEM parameters based on permuted data for comparisons, which yields a more realistic null for our comparisons, and that our

parameters are averaged over multiple repetitions of the IEM. These features should help mitigate errors due the peculiarities in the data at a given time point or sample of trials.

Data availability

The data that support the findings of this study are available from the corresponding author upon reasonable request.

Code availability

All custom code will be made available in a public repository on GitHub/OSF , please contact the corresponding author for more information.

Acknowledgments

We would like to thank James Elliott for his crucial feedback and suggestions, as well as Caroline Trinh, Lena Nalbandian, and Scott Patterson for their help with data collection. This work was supported by the Institute for Collaborative Biotechnologies through grant W911NF-09-0001 from the U.S. Army Research Office. The content of the information does not necessarily reflect the position or the policy of the Government, and no official endorsement should be inferred.

Author Contributions

M.H.M. and T.B. are co-first authors. M.H.M, T.B., and B.G. designed the experiment. T.B. programmed the experiment. M.H.M and T.B. collected the data. T.B. and M.H.M. analyzed the data. M.H.M, T.B., and B.G. wrote the manuscript.

Declaration of Interests

The authors declare no competing interests.

References

Awh, E., Jonides, J., & Reuter-Lorenz, P. A. (1998). Rehearsal in spatial working memory. *Journal of Experimental Psychology: Human Perception and Performance*, *24*(3), 780–790. http://doi.org/10.1037/0096-1523.24.3.780

Awh, E., Jonides, J., Smith, E. E., Buxton, R. B., Frank, L. R., Love, T., … Gmeindl, L. (1999). Rehearsal in Spatial Working Memory: Evidence From Neuroimaging. *Psychological Science*, *10*(5), 433–437. http://doi.org/10.1111/1467-9280.00182

Barry, R. J., Clarke, A. R., Johnstone, S. J., Magee, C. A., & Rushby, J. A. (2007). EEG differences between eyes-closed and eyes-open resting conditions. *Clinical Neurophysiology*, *118*, 2765–2773. http://doi.org/10.1016/j.clinph.2007.07.028

Brouwer, G. J., & Heeger, D. J. (2009). Decoding and Reconstructing Color from Responses in Human Visual Cortex. *Journal of Neuroscience*, *29*(44), 13992–

14003. http://doi.org/10.1523/JNEUROSCI.3577-09.2009

Brouwer, G. J., & Heeger, D. J. (2011). Cross-orientation suppression in human visual cortex. *Journal of Neurophysiology*, *106*(5), 2108–19. http://doi.org/10.1152/jn.00540.2011

Brouwer, G. J., & Heeger, D. J. (2013). Categorical Clustering of the Neural Representation of Color. *Journal of Neuroscience*, *33*(39), 15454–15465. http://doi.org/10.1523/JNEUROSCI.2472-13.2013

Bullock, T., Elliott, J. C., Serences, J. T., & Giesbrecht, B. (2017). Acute Exercise Modulates Feature-selective Responses in Human Cortex. *Journal of Cognitive Neuroscience*, *29*(4), 605–618. http://doi.org/10.1162/jocn_a_01082

Chapman, R. M., Armington, J. C., & Bragdon, H. R. (1962). A quantitative survey of kappa and alpha EEG activity. *Electroencephalography and Clinical Neurophysiology*, *14*(6), 858–868. http://doi.org/10.1016/0013-4694(62)90136-0

Chun, M. M., Golomb, J. D., & Turk-Browne, N. B. (2011). A Taxonomy of External and Internal Attention. *Annual Review of Psychology*, *62*(1), 73–101. http://doi.org/10.1146/annurev.psych.093008.100427

de Munck, J. C., Gonçalves, S. I., Huijboom, L., Kuijer, J. P. A., Pouwels, P. J. W., Heethaar, R. M., & Lopes da Silva, F. H. (2007). The hemodynamic response of the alpha rhythm: An EEG/fMRI study. *NeuroImage*, *35*(3), 1142–1151. http://doi.org/10.1016/J.NEUROIMAGE.2007.01.022

Delorme, A., & Makeig, S. (2004). EEGLAB: an open source toolbox for analysis of single-trial EEG dynamics including independent component analysis. *Journal*

of Neuroscience Methods, *134*(1), 9–21. http://doi.org/10.1016/j.jneumeth.2003.10.009

Di Russo, F., Martínez, A., & Hillyard, S. A. (2003). Source Analysis of Event-related Cortical Activity during Visuo-spatial Attention. *Cerebral Cortex*, *13*(5), 486–499. http://doi.org/10.1093/cercor/13.5.486

Dienes, Z. (2016). How Bayes factors change scientific practice. *Journal of Mathematical Psychology*, *72*, 78–89. http://doi.org/10.1016/j.jmp.2015.10.003

Ester, E. F., Sprague, T. C., & Serences, J. T. (2015). Parietal and Frontal Cortex Encode Stimulus-Specific Mnemonic Representations during Visual Working Memory. *Neuron*, 1–13. http://doi.org/10.1016/j.neuron.2015.07.013

Foster, J. J., Sutterer, D. W., Serences, J. T., Vogel, E. K., & Awh, E. (2016). The topography of alpha-band activity tracks the content of spatial working memory. *Journal of Neurophysiology*, *115*(1), 168–77. http://doi.org/10.1152/jn.00860.2015

Foster, J. J., Sutterer, D. W., Serences, J. T., Vogel, E. K., & Awh, E. (2017). Alpha-Band Oscillations Enable Spatially and Temporally Resolved Tracking of Covert Spatial Attention. *Psychological Science*, *28*(7), 929–941. http://doi.org/10.1177/0956797617699167

Garcia, J. O., Srinivasan, R., & Serences, J. T. (2013). Near-real-time feature-selective modulations in human cortex. *Current Biology*, *23*(6), 515–522. http://doi.org/10.1016/j.cub.2013.02.013

Gelman, A., & Tuerlinckx, F. (2000). Type S error rates for classical and Bayesian single and multiple comparison procedures. *Computational Statistics*, *15*(3),

373–390. http://doi.org/10.1007/s001800000040

Gomez-Herrero, G., Clercq, W., Anwar, H., Kara, O., Egiazarian, K., Huffel, S., & Paesschen, W. (2006). Automatic Removal of Ocular Artifacts in the EEG without an EOG Reference Channel. *Proceedings of the 7th Nordic Signal Processing Symposium - NORSIG 2006*, 130–133. http://doi.org/10.1109/NORSIG.2006.275210

Harrison, S. A., & Tong, F. (2009). Decoding reveals the contents of visual working memory in early visual areas. *Nature*, *458*(7238), 632–5. http://doi.org/10.1038/nature07832

Hillyard, S. A., Martínez, A., Anllo-Vento, L., Sereno, M. I., Frank, L. R., Buxton, R. B., … Heinze, H. J. (1999). Involvement of striate and extrastriate visual cortical areas in spatialattention. *Nature Neuroscience*, *2*(4), 364–369. http://doi.org/10.1038/7274

Kass, R. E., & Raftery, A. E. (1995). Bayes Factors. *Journal of the American Statistical Association*, *90*(430), 773–795. http://doi.org/10.1080/01621459.1995.10476572

Kelly, S. P., Lalor, E. C., Reilly, R. B., & Foxe, J. J. (2006). Increases in Alpha Oscillatory Power Reflect an Active Retinotopic Mechanism for Distracter Suppression During Sustained Visuospatial Attention. *Journal of Neurophysiology*, *95*(6). Retrieved from http://jn.physiology.org/content/95/6/3844.short

King, J.-R., & Dehaene, S. (2014). Characterizing the dynamics of mental representations: the temporal generalization method. *Trends in Cognitive Sciences*, *18*(4), 203–10. http://doi.org/10.1016/j.tics.2014.01.002

Kiyonaga, A., & Egner, T. (2013). Working memory as internal attention: Toward an integrative account of internal and external selection processes. *Psychonomic Bulletin & Review*, *20*(2), 228–242. http://doi.org/10.3758/s13423-012-0359-y

Kruschke, J. K., & Liddell, T. M. (2016). The Bayesian New Statistics : Hypothesis testing , estimation , meta-analysis , and planning from a Bayesian perspective. *Psychonomic Bulletin & Review*, 1–53. http://doi.org/http://dx.doi.org/10.2139/ssrn.2606016

Lewis-Peacock, J. A., Drysdale, A. T., Oberauer, K., & Postle, B. R. (2012). Neural Evidence for a Distinction between Short-term Memory and the Focus of Attention. *Journal of Cognitive Neuroscience*, *24*(1), 61–79. http://doi.org/10.1162/jocn_a_00140

Morey, R. D., Rouder, J. N., & Jamil, T. (2015). Package "Bayes Factor".

Naselaris, T., Kay, K. N., Nishimoto, S., & Gallant, J. L. (2011). Encoding and decoding in fMRI. *NeuroImage*, *56*(2), 400–410. http://doi.org/10.1016/j.neuroimage.2010.07.073

Pearson, D., & Sahraie, A. (2003). Oculomotor control and the maintenance of spatially and temporally distributed events in visuo-spatial working memory. *The Quarterly Journal of Experimental Psychology Section A*, *56*(7), 1089–1111. http://doi.org/10.1080/02724980343000044

Postle, B. R., Awh, E., Jonides, J., Smith, E. E., & D'Esposito, M. (2004). The where and how of attention-based rehearsal in spatial working memory. *Cognitive Brain Research*, *20*(2), 194–205. http://doi.org/10.1016/J.COGBRAINRES.2004.02.008

Rouder, J. N., Morey, R. D., Speckman, P. L., & Province, J. M. (2012). Default Bayes factors for ANOVA designs. *Journal of Mathematical Psychology*, *56*(5), 356–374. http://doi.org/10.1016/j.jmp.2012.08.001

Samaha, J., Sprague, T. C., & Postle, B. R. (2016). Decoding and Reconstructing the Focus of Spatial Attention from the Topography of Alpha-band Oscillations. *Journal of Cognitive Neuroscience*, *28*(8), 1090–1097. http://doi.org/10.1162/jocn_a_00955

Serences, J. T., Ester, E. F., Vogel, E. K., & Awh, E. (2009). Stimulus-Specific Delay Activity in Human Primary Visual Cortex. *Psychological Science*, *20*(2), 207–214. http://doi.org/10.1111/j.1467-9280.2009.02276.x

Serences, J. T., & Saproo, S. (2012). Computational advances towards linking BOLD and behavior. *Neuropsychologia*, *50*(4), 435–446. http://doi.org/10.1016/j.neuropsychologia.2011.07.013

Sprague, T. C., Ester, E. F., & Serences, J. T. (2016). Restoring Latent Visual Working Memory Representations in Human Cortex. *Neuron*, *91*(3), 694–707. http://doi.org/10.1016/j.neuron.2016.07.006

Suchow, J. W., Brady, T. F., Fougnie, D., & Alvarez, G. A. (2013). Modeling visual working memory with the MemToolbox. *Journal of Vision*, *13*(10), 9–9. http://doi.org/10.1167/13.10.9

Thut, G., Nietzel, A., Brandt, S. a, & Pascual-Leone, A. (2006). Alpha-band electroencephalographic activity over occipital cortex indexes visuospatial attention bias and predicts visual target detection. *The Journal of Neuroscience : The Official Journal of the Society for Neuroscience*, *26*(37), 9494–502.

http://doi.org/10.1523/JNEUROSCI.0875-06.2006

van Moorselaar, D., Foster, J. J., Sutterer, D. W., Theeuwes, J., Olivers, C. N. L., & Awh, E. (2018). Spatially Selective Alpha Oscillations Reveal Moment-by-Moment Trade-offs between Working Memory and Attention. *Journal of Cognitive Neuroscience*, *30*(2), 256–266. http://doi.org/10.1162/jocn_a_01198

Wetzels, R., Matzke, D., Lee, M. D., Rouder, J. N., Iverson, G. J., & Wagenmakers, E.-J. (2011). Statistical Evidence in Experimental Psychology. *Perspectives on Psychological Science*, *6*(3), 291–298. http://doi.org/10.1177/1745691611406923

Wilken, P., & Ma, W. J. (2004). A detection theory account of change detection. *Journal of Vision*, *4*(12), 11. http://doi.org/10.1167/4.12.11

Worden, M. S., Foxe, J. J., Wang, N., & Simpson, G. V. (2000). Anticipatory biasing of visuospatial attention indexed by retinotopically specific alpha-band electroencephalography increases over occipital cortex. *The Journal of Neuroscience : The Official Journal of the Society for Neuroscience*, *20*(6), RC63. Retrieved from http://www.ncbi.nlm.nih.gov/pubmed/10704517

Zhang, W., & Luck, S. J. (2008). Discrete fixed-resolution representations in visual working memory. *Nature*, *453*(7192), 233–235. http://doi.org/10.10

Supplementary Information

To what extent can the spatially selective responses and modulations of temporal generalizability be attributed to stimulus-evoked potentials? It is possible that the spatially selective responses observed in the post-target period are driven by the visually evoked potential to the initial stimulus. As a result, losses in temporal generalizability could be attributed to the transient nature of the evoked potential. To test this possibility, we used the topography of the target-evoked potential (P1) to train the IEM, and then tested the model on alpha band power at each time point. The P1 component was determined by locating the latency of the peak amplitude in parietal and parietal/occipital electrodes between 100 and 180 ms for each subject and condition, and then averaging across 3 samples either side of the peak (+/- 11.72 ms) to obtain the mean amplitude. This model was able to capture spatially-selective responses (*Fig. S1a,b*), although they were less robust than those trained and tested within alpha (*Fig. S1c*). This is not in opposition to any of the arguments we outline in our paper. We fully endorse the possibility that the P1 and alpha oscillations are two indicators of the same early visual processing that encodes location information. However, our additional analyses show that a model trained on the target-evoked P1 can also derive spatially-selective responses in alpha oscillations well into the retention interval, even in the eyes-closed condition. Thus, again, it is unlikely that losses in temporal generalization from early points forward in time are solely due to the evoked response confounding the signal in the frequency domain.

Does added alpha power from eye closure, unrelated to the alpha that encodes location, cause the loss of temporal generalization observed in the eyes closed conditions? Closing the eyes tends to result in an increase in alpha power, particularly at posterior electrodes. It is reasonable to suppose that this systematic perturbation of alpha power and topography caused the loss of generalization in the eyes closed condition. In order to examine this possibility, we again ran the IEM and the temporal generalization analysis for the eyes open conditions, but prior to modeling we added alpha power to simulate the increase in alpha power observed in the eyes closed condition. Specifically, to each electrode, at each sample from 750 (deadline for eye closure)-2,000 ms after target onset, we added random alpha power sampled from a normal distribution with the mean of the difference in power between the eyes closed and eyes open conditions, and the pooled standard deviation of power in the eyes open and eyes closed conditions for that electrode at that sample. This added noise then reflects the difference in alpha power between the eyes open and eyes closed condition for that particular electrode site and includes the systematic differences in alpha topography between the conditions. In other words, the added noise reflects the exact changes in alpha power and topography between the eyes closed and eyes open conditions. However, as the noise is drawn randomly from the distribution of difference in power and topography between eyes open and eyes closed conditions this noise should not impact the temporal generalization of the spatially selective representation. This is necessary as the spatially selective representation extracted with the IEM is based on the pattern of alpha that is predicted by the *a priori* defined set of spatially

selective neural channels ("basis set"). In order for any change to alpha power or topography to affect the results of the IEM, and its generalization, it must necessarily impact the relationship between the pattern of alpha power and the basis set. Changes that are independent of the pattern of alpha that codes the spatially selective representation will not affect the result of the IEM or its generalization.

Consistent with this line of reasoning, alpha power in the eyes open conditions with the added noise resembled that in the eyes closed condition (*Fig. S2a*). The topography of alpha power in the eyes open conditions with the additional noise also closely resembles that of the corresponding eyes closed condition during the 750-2,000 ms period (*Fig. S2b*). The results of the temporal generalization of the IEM in the eyes open conditions (both with and without mask) with the added power were identical to that observed without the added power (*Fig. S2c*). Again, this finding is consistent with our argument that in order for the change in alpha power that accompanies eyes closure to affect the results of the IEM and the temporal generalization of the IEM, it would have to interact with the specific pattern of alpha power that encodes location.

What is different between process 1 and process 2? Within the context of the analytical approach, the answer to this question is that the pattern of weights across electrodes generated by the IEM differs between process 1 and process 2 in the eyes closed conditions, but not within process 1 and process 2. Indeed in the eyes open condition there is a single time window during which there is no consistent change, beginning at ~300 ms after target onset – corresponding to process 1 (*Fig. S3a*). In contrast, in the eyes closed condition there are two separate time windows during which there is no consistent change in weights: the first from ~300 to 900 ms after target onset, and the other from ~900 to 2,000 ms (*Fig. S3b*). These two time periods roughly correspond to the two processes evident in the temporal generalization of the IEM. From the first time window, possibly equating to process 1, to the second time window, possibly equating to process 2, weights on average moved in the negative direction. Overall, weights are more dynamic, showing greater absolute weight change over time, in the eyes closed conditions (*Fig. S3c*), but especially during the retention interval, than in the eyes open conditions (*Fig. S3d*). In order to examine the topography of the change in weights over time during the retention interval we ranked the electrodes according to absolute change in weight between the two time points of every sample pair in the temporal generalization matrix. We then averaged these rankings over the generalization matrix during the period from 750-2,000 ms. For both eyes open and eyes closed conditions parietal and occipital electrode sites were consistently ranked highest for weight change (*Fig. S3e*). These electrodes also consistently rank highest in terms of absolute weight in the IEM (*Fig. S3f*).

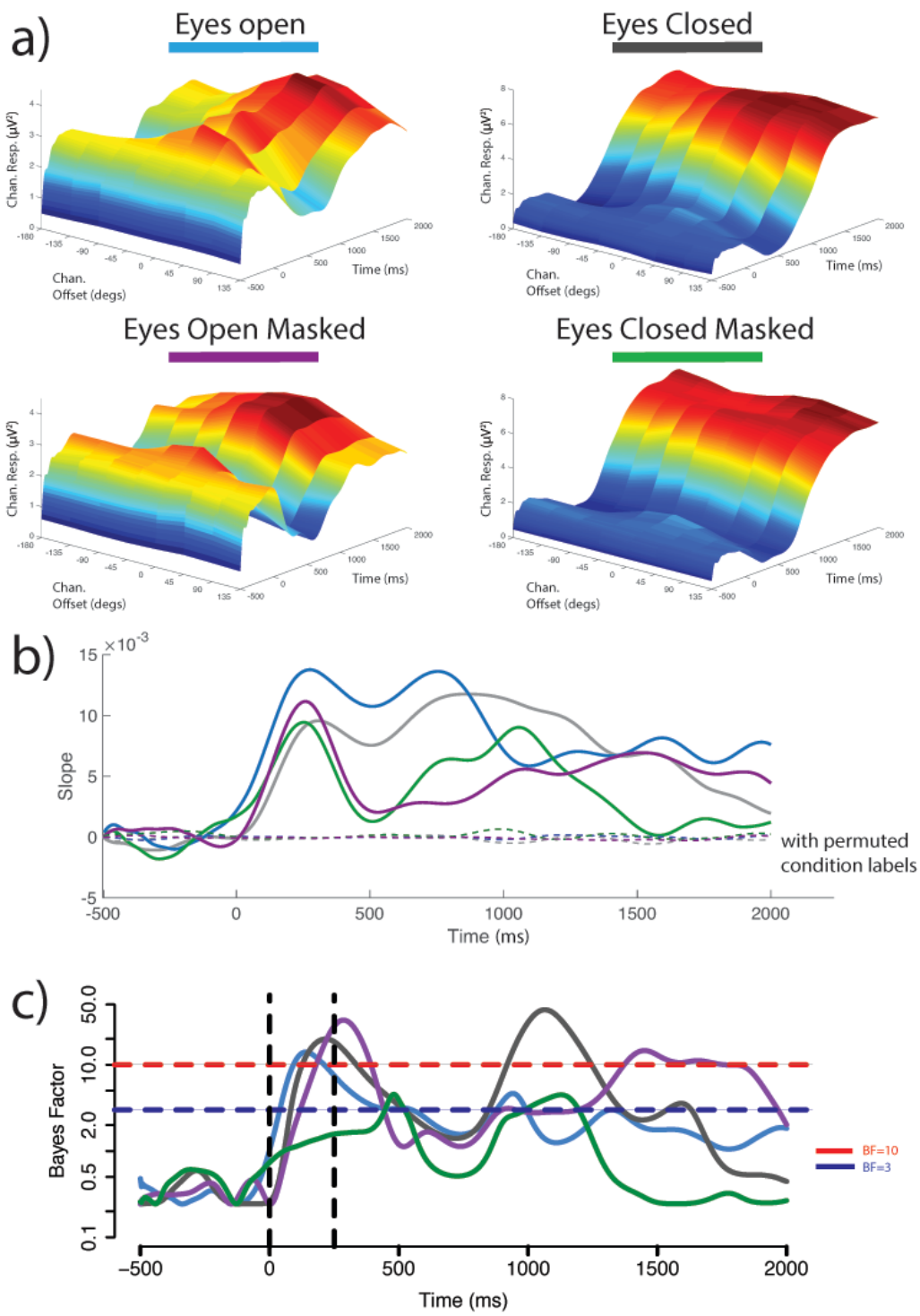

Fig. S1. Results from training the IEM on the stimulus-evoked event related potential (P1) and testing on Alpha power at each time point. (a) Estimated neural population response, or "channel" (offset of channel's preferred location from stimulus location: ±0,45,90,135, or 180°), response (alpha-band power) starting 500 ms before onset of stimulus until end of retention period. (b) Linear regression weights of estimated channel response folded around 0° offset ("slope"), indicating the degree of spatial selectivity. (c) Bayes Factor (BF)

of t-test comparing slope at each time point to slope of response estimated using permuted location labels.

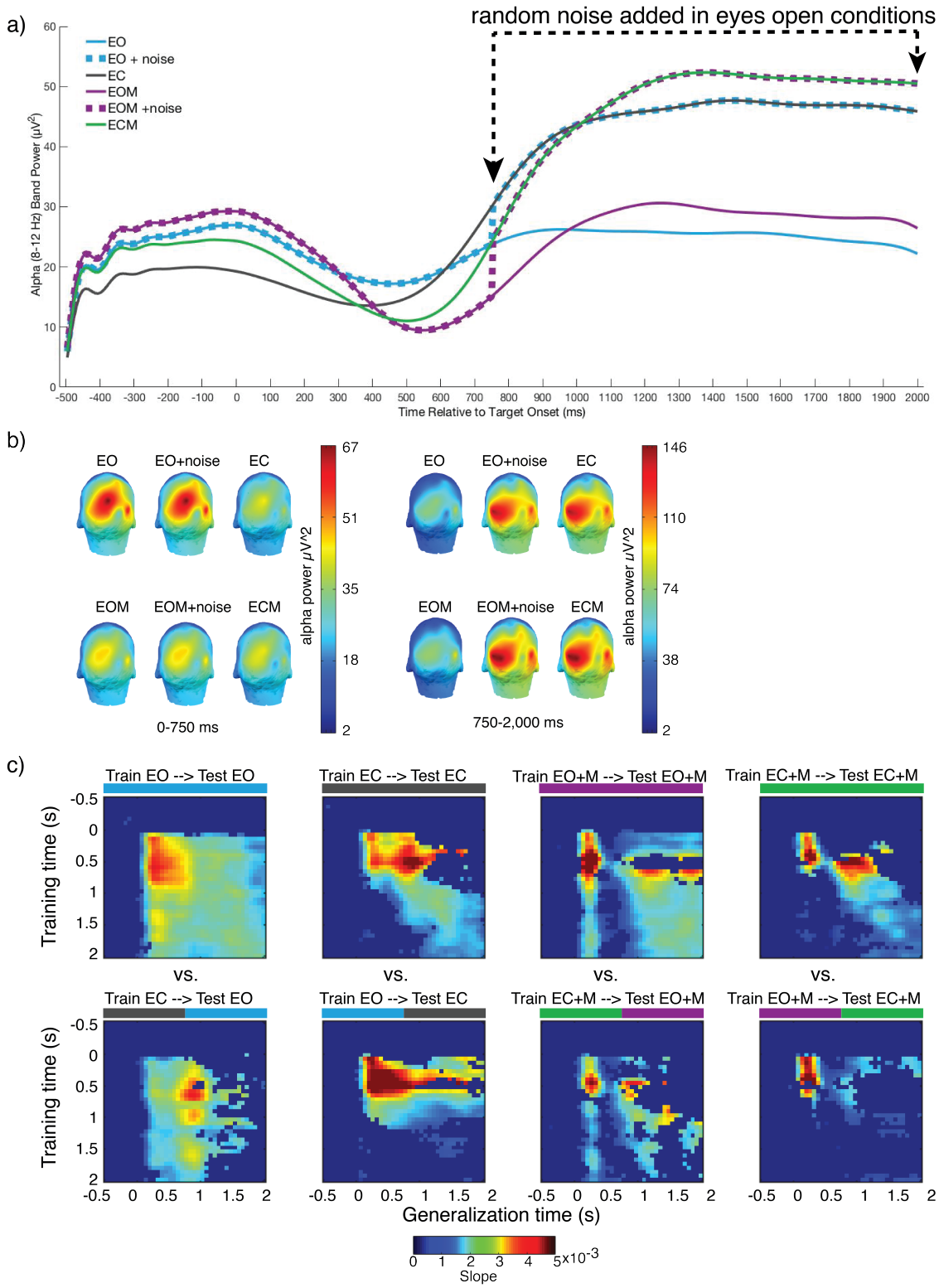

Fig. S2. a) Mean alpha power averaged across all electrodes. Power in the eyes open conditions with the added noise follows that in the corresponding eyes closed conditions exactly. b) Topography (occipital view) of mean alpha power averaged across two time windows: 0-750 ms, and 750-2,000 ms after target onset. c) Temporal generalization analysis using eyes open conditions with added noise.

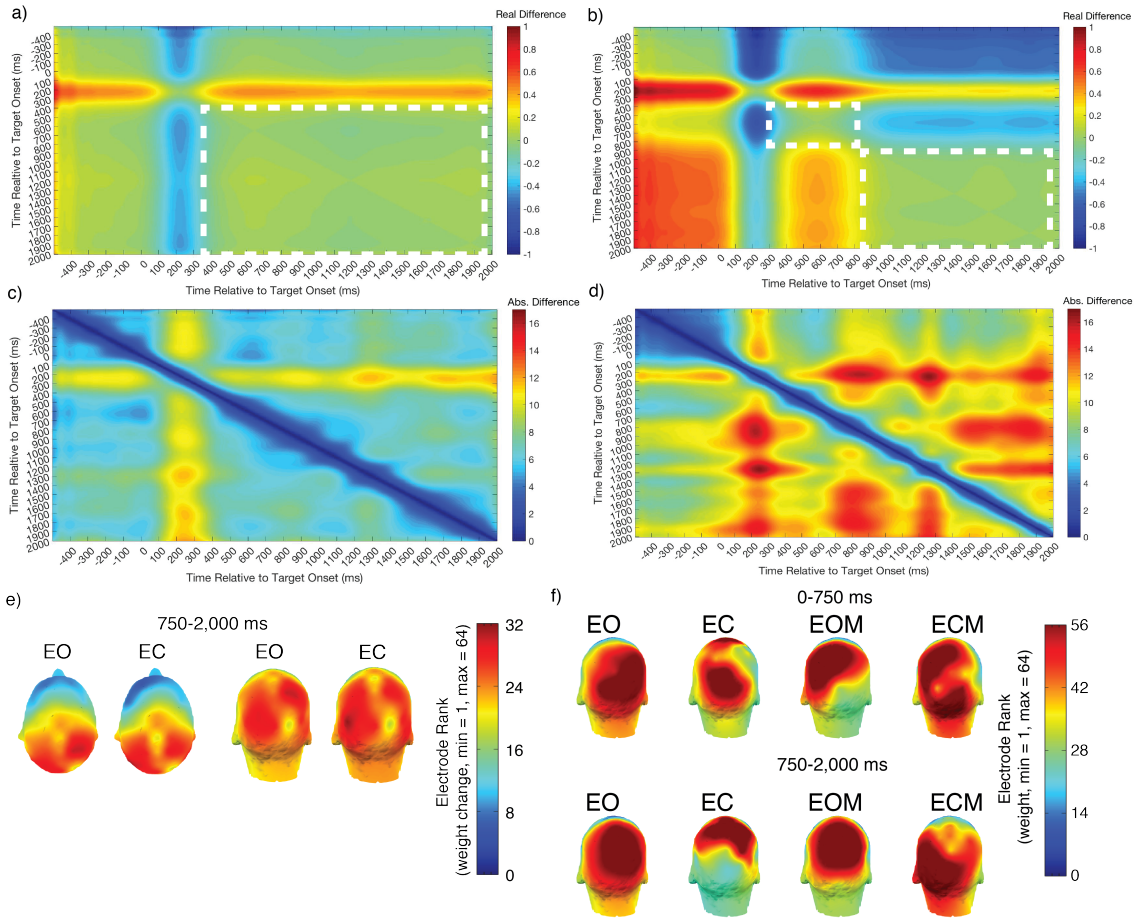

Fig. S3. a) Change in IEM weights (t2-t1) averaged across all channels and electrodes in the EO condition. Note that the change in weights averages to ~ 0 (green) for all samples beginning ~ 300 ms to 2,000 ms (end of retention interval) after stimulus onset (outlined in dashed white line). Consistent change is seen in the weights from those samples that overlap with the stimulus-evoked potentials (~0-300 ms), the weights of which tend to change in a positive direction for all later samples. b) Change in weights (t2-t2) averaged across all channels and electrodes in the EC condition. As with the EO condition consistent weight change is seen in the weights from those samples that overlap with the stimulus-evoked potentials (~0-300 ms), the weights of which tend to change in a positive direction for all later samples. Note that there are two periods (outlined with dashed white line) where the average weight change is ~ 0 (green): (1) ~300-900 ms and (2) ~900-2,000 ms after stimulus onset. From (1) to (2) there is consistent weight change in the negative direction. c) *Absolute* change in weights (t2-t1) averaged across all channels and electrodes in the EO condition. d) *Absolute* change in weights (t2-t1) averaged across all channels and electrodes in the EC condition. e) Topography of mean electrode rank of weight change. Higher values indicate that an electrode was consistently ranked higher in terms of amount of absolute weight change across all channels during the period from 750-2,000 ms after stimulus onset. Both parietal and occipital electrodes were consistently ranked higher in terms of weight change during that period for both EO and EC conditions. f) Topography of mean electrode rank of weight. Higher values indicate that an electrode was consistently ranked higher in terms of weight across all channels.